BUCK/BOOST CONVERTER WITH IVFF TECHNIQUE FOR CONTROLLING VSC OF AN INDUCTION MOTOR DRIVE

P.CHAITANYA THEJA, M.Tech scholar
EEE DEPARTMENT, SIETK
PUTTUR, INDIA
chaitanyatheja.p@gmail.com

C.R.HEMAVATHI
Asst. professor, EEE DEPARTMENT
SIETK,PUTTUR, INDIA
sietkeee.tp@gmail.com

Abstract:-In recent years the use of buck-boost converters are more when compared to other type of converters. When compared with the basic converters like cuk, zeta the two switch buck-boost converter (TSBB) presents less voltage losses on the switches. The two switch buck-boost converter requires fewer passive components can effectively reduce the conduction and switching losses, leading to high efficiency over a wide input voltage range. The TSBB converters has been extensively used in telecommunications, battery operated vehicles etc. with wide input voltage range. So it is thus important to improve the efficiency of TSBB converter over a high input voltage range. So in the telecommunications systems and fuel cells the TSBB converter input voltage fluctuates with output power, due to the input voltage response is not satisfactory. If the input transient voltage response is not satisfactory it creates problems on the output response of the system. so in addition to these TSBB converter we use input voltage feed forward method (IVFF) to improve the input transient response and reduces the effect of input voltage disturbances on the output of the system. These input voltage feed forward compensation is then proposed for two switch buck boost converter which realizes the automatic selections of operating modes and input voltage feed forward functions. The smooth switching between boost and buck modes is guaranteed with inverting mode of operation for the control of induction motor by representing its characteristics using matlab/simulink.

Index Terms—*Input voltage feed-forward, small-signal model, two-mode control, two-switch buck-boost converter , induction motor,multi level inverter(MLI).*

I. INTRODUCTION

THE two-switch buck-boost (TSBB) converter, as shown in Fig. 1, is a simplified cascade connection of buck and boost converters [1]. Compared with the basic converters, which have the ability of both voltage step-up and step-down, such as inverting buck-boost, Cuk, Zeta, and SEPIC converters, the TSBB converter presents lower voltage stress of the power devices, fewer passive components, and positive output voltage [2]–[4], and it has been widely used in telecommunication systems [4], battery-powered power supplies [5], [6], fuel-cell power systems [7], [8], power factor correction (PFC) applications [9], [10], and raido frequency (RF) amplifier power supplies [11], all of which have wide input voltage range. It is thus imperative for the TSBB converter to achieve high efficiency over the entire voltage range. Moreover, considering that the input voltages from battery and fuel cell fluctuate with the output power, and the input voltage in the PFC applications varies with the sinusoidal line voltage, a satisfactory input transient response preventing large output votlage variation in case of input voltage variation is also desired for the TSBB converter. There are two active switches in the TSBB converter, which provides the possibility of obtaining various control methods for this converter. If $Q1$ and $Q2$ are switched ON and OFF simultaneously, the TSBB converter behaves the same as the single switch buck-boost converter. This control method is called one mode control scheme [12], [13]. Q_1 and Q_2 can also be controlled in other manners. For example, when the input voltage is higher than the output voltage, Q_2 is always kept OFF, and Q_1 is controlled to regulate the output voltage, and as a result, the TSBB converter is equivalent to a buck converter, and is said to operate in *buck mode*. On the other hand, when the input voltage is lower than the output voltage, Q_1 is always kept ON, and Q_2 is controlled to regulate the output voltage, and in this case, the TSBB converter is equivalent to a boost converter, and is said to operate in *boost mode*. Such control method is called two-mode control scheme [3], [4]. Compared with one-mode control scheme, two-mode control scheme can reduce the conduction loss and switching loss effectively, leading to a high efficiency over a wide input voltage range, as explained in [4]. Besides, in order to achieve automatic switching between buck and boost modes, the two-mode control scheme based on two modulation

signals with one carrier or one modulation signal with two carriers was proposed in [14].

When the TSBB converter operates in continuous current boost mode, it presents a right-half-plane (RHP) zero. This RHP zero limits the bandwidth of the control loop, penalizing the transient response [15].

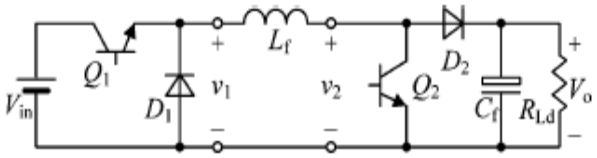

Fig. 1. Two-switch buck-boost (TSBB) converter.

Moreover, in the two-mode control scheme with automatic mode-switching, only one voltage regulator is used for both buck and boost modes, and it is often designed to have enough phase margin in boost mode by reducing the bandwidth of the control loop, thus the transient responses of this converter are deteriorated in the whole input voltage range, including both buck and boost modes. To improve the transient response of the TSBB converter, average current mode control [16], current-programmed mode control [17], [18], and voltage mode control with a two-mode proportional-integral derivative (PID) [19], Type-III (2–zeros and 3–poles) [20] compensator, or passive *RC*-type damping network [21] are employed. With these control schemes mentioned earlier, the influence of the input voltage and load disturbances on the output voltage can be well reduced, but cannot be fully eliminated. For the converter in the applications with wide input voltage variation, input voltage feed-forward (IVFF) compensation is an attractive approach for improving the transient response of the converter, for it can eliminate the effect of the input voltage disturbance on the output voltage in theory. The IVFF of the buck or boost converter can be implemented in several methods:

1) vary either the amplitude of the carrier signal [22], [23] or the value of the modulation signal [24]–[26] according to the input voltage. However, the variations of the carrier signal for the IVFF of the boost converter and the modulation signal for IVFF of the buck converter are both inversely proportional to the input voltage, which imply that the implementation of this IVFF method is complicated relatively for the TSBB converter.

2) Calculate the duty ratio [27]–[30]. Since the duty ratio calculation for the buck converter is inversely proportional to the input voltage, a little complicated realization is also required.

3) Derive the IVFF function producing zero audio susceptibility through the small-signal model [31]–[34]. As derived in [31], the IVFF functions of buck and boost converters are both in proportion to the input voltage, and they are easy to be implemented. So, the IVFF method with derived IVFF function from the small-signal model will be adopted in this paper.

IVFF compensation for the TSBB converter with two-mode control scheme has been achieved by varying the peak and valley values of the carrier signal in proportion to the input voltage in buck and boostmodes, respectively [35], or the peak value of the carrier signal and modulation signal in proportion to input voltage simultaneously [36]. In these control schemes, the selection and switching of operating modes and IVFF compensations are not automatic, but require a rather complicated mode detector, which is realized by comparing the input voltage and output voltage and adding auxiliary circuits. In addition, considering the carrier signal generators of most IC-controllers operate from an internally derived power supply, the IVFF methods by vary varying the carrier signal with input voltage are not very general. Thus, this paper will combine the two-mode control scheme with automatic mode-switching ability and the IVFF functions derived from the small-signal models under different operating modes together, and propose a general, easy implementation, and effective two-mode scheme with IVFF compensation, achieving automatic selections of the operating modes and the corresponding IVFF functions simultaneously. In other words, when the input voltage is higher than the output voltage, the TSBB converter with this proposed control scheme can operate in buck mode and select the IVFF function of this mode automatically. On the other side, when the input voltage is lower than the output voltage, the TSBB converter can operate in boost mode and select the IVFF function of boost mode automatically. This paper is organized as follows. Section II introduces the two-mode control scheme with automatic mode-switching ability for the TSBB converter, and Section III derives its small signal models under different operating modes. Based on the derived small-signal models, the IVFF functions under different operating modes are derived, and a two-mode control scheme with IVFF compensation is proposed to achieve automatic selections of operating modes and the corresponding IVFF functions simultaneously, and nearly smooth mode-switching. Besides, the comparisons between the two-mode control scheme with and without IVFF compensation are given in Section IV. Section V presents the experimental results from a prototype with this proposed control scheme, and finally, Section VI concludes this paper.

II. TWO-MODE CONTROL SCHEME WITH AUTOMATIC MODE-SWITCHING ABILITY

As shown in Fig. 1, the voltage conversion of the TSBB converter operated in continuous current mode (CCM) is [4]

$$V_0=\frac{d_1}{1-d_2}V_{in} \quad (1)$$

where d_1 and d_2 are the duty cycles of switches Q_1 and Q_2 , respectively. In the two-mode control scheme, d_1 and d_2 are controlled independently. When the input voltage is higher than the output voltage, the TSBB converter operates in *buck mode*, where d_2 = 0, i.e., $Q2$ is always OFF, and d_1 is controlled to regulate the output voltage; when the input voltage is lower than the output voltage, the TSBB converter operates in *boost mode*, where d_1 = 1, i.e., Q_1 is always ON, and d_2 is controlled to regulate the output voltage. Thus, the voltage conversion of the TSBB converter with two-mode control scheme can be written as Fig. 2 shows the TSBB converter under the two-mode control scheme based on two modulation signals and one carrier, and Fig. 3 gives the

$$V_0=\begin{cases} d_1V_{in}, & d_2=0(V_{in}\geq V_0) \\ \frac{V_{in}}{1-d_2}, & d_1=0(V_{in}<V_0) \end{cases} \quad (2)$$

key waveforms of this control scheme, where $v_{e\text{-buck}}$ and $v_{e\text{- boost}}$ are the modulation signals of Q_1 and Q_2 , respectively, and v_{saw} is the carrier. The maximum and minimum values of the carrier are *VH* and *VL* , respectively, and

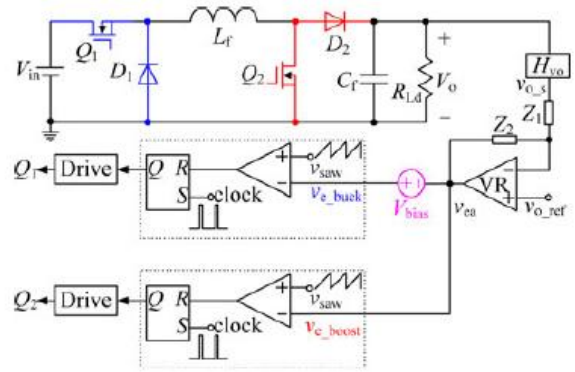

Fig. 2. TSBB converter under the two-mode control scheme

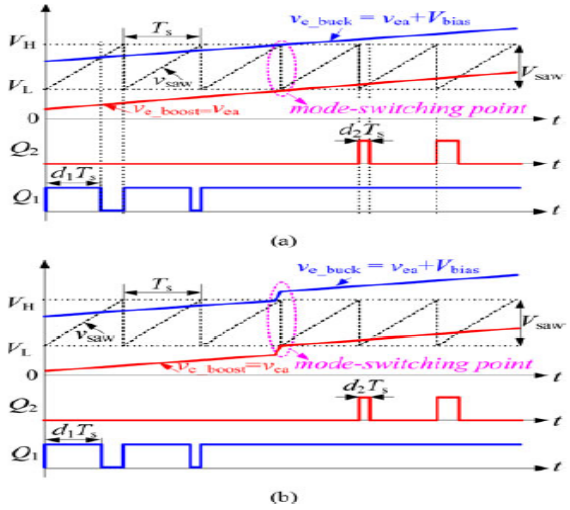

Fig. 3. Two-mode control scheme based on two modulation signals and one carrier.
(a) $V_{bias} = V_{saw}$. (b) $V_{bias} > V_{saw}$.

the peak-to-peak value of the carrier is $V_{saw} = V_H - V_L$. With the same carrier, in order to achieve the two-mode operation as described in (2), only one of $v_{e\text{-buck}}$ and $v_{e\text{-boost}}$ can intersect v_{saw} at any time. So, it is required that

$$v_{e\text{-buck}} - v_{e\text{-boost}} \geq v_{saw} \quad (3)$$

$$\begin{cases} v_{e-\text{buck}} = V_{ea} + V_{bias} \\ v_{e-\text{b00st}} = V_{ea} \end{cases} \quad (4)$$

Substituting (4) into (3) yields

$$V_{bias} \geq V_{saw}. \quad (5)$$

So, the modulation signal in (4) with $V_{bias} \geq V_{saw}$ can achieve the two-mode operation of the TSBB converter. When $V_{in} > V_o$, $v_{e\text{-buck}}$ will be within [V_L, V_H], and it intersects v_{saw} and thus determines $d1$; and meanwhile, ve boost = $vea \leq ve$ buck $- V_{saw} < V_L$, and thus d_2 = 0. Such case corresponds to the buck mode of the TSBB converter. When $Vin < Vo$, $v_{e\text{-boost}} = v_{ea}$ will be within [V_L, V_H], and it intersects $vsaw$ and thus determines d_2 ; and meanwhile, $v_{e\text{- buck}} = v_{ea} + V_{bias} \geq vea + V_{saw} > V_H$, and thus d_1 = 1. Such case corresponds to the boost mode of the TSBB converter. When $V_{in} = V_o$, which is the switching point of the buck and boost modes, $v_{e\text{-boost}} = V_L$, and thus d_2 = 0; and meanwhile, $v_{e\text{-buck}} \geq V_H$, and thus d_1 = 1. It can be found that $v_{e\text{-buck}} = V_H$ if $V_{bias} = V_{saw}$, and $v_{e\text{-buck}} > V_H$ if $V_{bias} > V_{saw}$ at the mode-switching point, as depicted in Fig. 3(a) and (b), respectively. So, by letting $V_{bias} = V_{saw,}$ i.e., $v_{e\text{-buck}} - v_{e\text{-boost}} = V_{saw}$ at the mode-switching point, the buck and boost modes can be smoothly switched from each other.

III. IVFF FOR TWO-MODE CONTROL SCHEME

A. Derivations of DC and Small-Signal Models of the TSBB Converter

As described in [37] and [38], in the averaged switch model of a dc–dc converter, the switch is modeled by a controlled current source with the value equaling to the average current flowing through the switch, and the diode is modeled by a controlled voltage source with the value equaling to the average voltage across the diode. With this method, the averaged switch model of the TSBB converter can be obtained, as shown in Fig. 4(a), where $iQ_1 = d_1\, iL$ and $iQ_2 = d_2\, i_L$, which are the average currents flowing through switches Q_1 and Q_2 , respectively, and $vD_1 = d1vin$ and $vD_2 = d_2v_o$, which are the average voltages across diodes D_1 and D_2 , respectively. The average values of voltage, current, and duty cycle in the averaged switch model can be decomposed into their dc and ac components, so iQ_1, iQ_2, vD_1 , and vD_2 can be expressed as

$$\begin{aligned} iQ_1 &= iQ_{1+}\hat{\imath}_{Q1}=(D_1+\hat{d}_1)(I_L+\hat{\imath}_L) \\ &= D_1 I_L + D_1\hat{\imath}_L+\hat{d}_1 I_L+\hat{d}_1\hat{\imath}_L \end{aligned} \quad (6)$$

$$iQ_2 = iQ_2 + \hat{\imath}_{Q2} = (D_2 + \hat{d}_2)(I_L + \hat{\imath}_L)$$
$$= D_2 I_L + D_2\hat{\imath}_L + \hat{d}_2 I_L + \hat{d}_2\hat{\imath}_L \quad (7)$$

$$vD_1 = vD_{1+}\hat{v}_{D1} = (D_1 + \hat{d}_1)(V_{in} + \hat{v}_{in})$$
$$= D_1 V_{in} + D_1\hat{v}_{in} + \hat{d}_1 V_{in} + \hat{d}_1\hat{v}_{in} \quad (8)$$

$$vD_1 = vD_{2+}\hat{v}_{D2} = (D_2 + \hat{d}_2)(V_0 + \hat{v}_0)$$
$$= D_2 V_0 + D_2\hat{v}_0 + \hat{d}_2 V_0 + \hat{d}_1\hat{v}_0 \quad (9)$$

Where the upper-case letter denotes the dc value, and the lowercase letter with hat (^) denotes the small-signal perturbation.

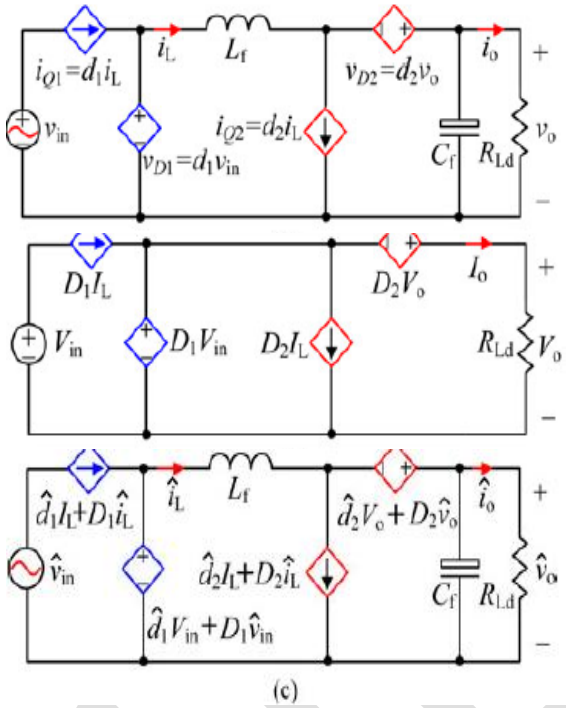

Fig. 4. Models of the TSBB converter. (a) Averaged switch model. (b) DC model. (c) Small-signal model.

With small-signal assumption, the average values in (6)–(9) can be linearized by neglecting the second-order ac terms [1]. Then, the dc model of the TSBB converter can be gotten by replacing the average values in Fig. 4(a) with the dc components in (6)–(9), as depicted in Fig. 4(b). Besides, the inductor L_f is short circuit, and the capacitor C_f is open circuit in the dc model. Likely, by replacing the average values in Fig. 4(a) with the first-order ac components in (6)–(9), the small-signal model of the TSBB converter can be obtained, as illustrated in Fig. 4(c). According to (2), setting $d_2 = 0$, i.e., $D_2 = 0$, $\hat{d}_2 = 0$, and $d_1 = 1$, i.e.,$D_1 = 1$, $\hat{d}_1 = 0$ in Fig. 4(c), respectively, the small-signal models in buck and boost modes can be derived.

B. Derivation of IVFF Functions

Fig. 5(a) shows a general control block diagram of a dc–dc converter [1], where $G_{vd}(s)$,G_{vo} v_{in} (s) and Z_o (s) are the transfer functions of the duty ratio $\hat{d}$, input voltage $\hat{V}_{in}$, and output current $\hat{\imath}_0$ to the output voltage $\hat{V}_0$, respectively, $G_v(s)$ is the transfer function of the voltage regulator ,$GPWM(s)$ is the transfer function of the pulse-width modulation (PWM) modulator, $\hat{v}_{o\text{-ref}}$ is the output voltage reference, and $H_{vo}(s)$ is the sense gain of the output voltage. As seen, the disturbance of input voltage $\hat{v}in$ affects the output voltage through the path with transfer function $G_{vo\text{-}vin}$ (s). This effect can be eliminated by introducing an additional path with transfer function $-G_{vo\text{-}vin}$ (s) from the input voltage to the output voltage, as illustrated with the dashed line shown in Fig. 5(a). Moving the output of $-G_{vo\text{-}vin}$ (s) to the output of voltage regulator and corresponding transfer function being changed to Gff (s), the control block is equivalently transformed to that shown in Fig. 5(b). The path from $\hat{V}_{in}$ to $\hat{V}_{ff}$ is called the IVFF path, and the IVFF

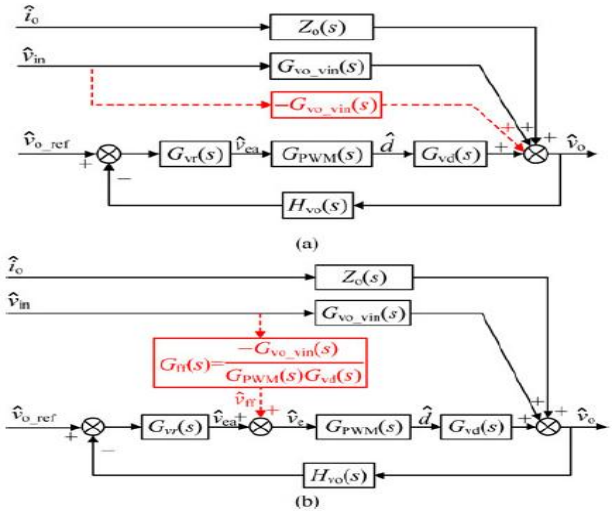

Fig. 5. Control block diagramwith IVFF of a dc–dc converter. (a) Introduction of IVFF.

(b) Equivalent transformation of IVFF.
function G_{ff} (s) is

$$G_{ff}(s) = \frac{\hat{v}_{ff}}{\hat{v}_{in}} = -\frac{G_{vo-vin}(s)}{G_{PWM}(s)G_{vd}(s)} \quad (10)$$

As shown in Fig. 5(b), the output of G_{ff} (s), i.e., $\hat{V}_{ff}$, is added to the output signal of the voltage regulator, i.e., v_{ea} , forming the modulation signal $\hat{V}_e$. As discussed earlier, by setting $D_2 = 0$ and $\hat{d}_2 = 0$ in the small-signal model of the TSBB converter shown in Fig. 4(c), the small-signal model in buck mode can be obtained, and the transfer functions of duty ratio and input voltage to the output voltage in this mode, $G_{vd\text{-}buck}(s)$ and $G_{vo\text{-}vin\text{-}buck}(s)$ can be derived as

$$G_{vd-buck}(s) = \frac{\hat{v}_0(s)}{\hat{d}(s)}\Big|_{\hat{v}_{in}=0} = \frac{v_{in-dc}}{s^2 L_f C_f + S\frac{L_f}{R_{Ld}} + 1} \quad (11)$$

$$G_{vo-vin-buck}(s)=\frac{\hat{v}_0(s)}{\hat{d}(s)}\Big|_{\hat{d}=0}=\frac{1}{s^2L_fC_f+S\frac{L_f}{R_{Ld}}+1}\ \frac{v_0}{v_{in-dc}} \quad (12)$$

Where L_f , C_f , and R_{Ld} are the filter inductor, filter capacitor, and load resistor of the TSBB converter, respectively, and $V_{\text{in-dc}}$ and V_o are the input voltage and output voltage at the quiescent operation point, respectively. Likewise, by setting $D_1 = 1$ and $\hat{d}_1 = 0$ in Fig. 4(c), the small-signal model in boost mode can be gotten, and the transfer functions of duty ratio and input voltage to the output voltage in this mode, $G_{vd\text{-boost}}(s)$ and $G_{vo\text{-}v\text{-in-boost}}(s)$, can be,

TABLE I
PARAMETERS OF THE PROTOTYPE

parameter	symbol	value
Input voltage	v_{in}	250-500V
Output voltage	V_o	360V
Output power	P_o	6KW
Full load resistor	R_{Ld}	21.6 Ω
Switching frequency	f_s	100HHZ
Switches	Q_1,Q_2	SPW47N60C3
Diodes	D_1,D_2	SDP30S120
Filter capacitor	C_f	4080μF
Filter inductor	L_f	320μH
Sense gain of the input voltage	H_{vin}	1/100
Sense gain of the output voltage	H_{vo}	1/144
Peak-to-peak value of the carrier	V_{saw}	2.5V

Respectively, derived as

$$G_{vd-buck}(s)=\frac{\hat{v}_0(s)}{\hat{d}(s)}\Big|_{\hat{v}_{in}=0}=\frac{1-S\frac{L_e}{R_{Ld}}}{s^2L_eC_f+S\frac{L_e}{R_{Ld}}+1}\ \frac{v_0^2}{v_{in-dc}} \quad (13)$$

$$G_{vo-vin-buck}(s)=\frac{\hat{v}_0(s)}{\hat{d}(s)}\Big|_{\hat{d}=0}=\frac{1}{s^2L_eC_f+S\frac{L_e}{R_{Ld}}+1}\ \frac{v_0}{v_{in-dc}} \quad (14)$$

Where $L_e = L_f v_0^2/v_{in-dc}^2$
The transfer function of the PWM modulator $G_{\text{PWM}}(s)$ can be expressed as [1]

$$G_{\text{PWM}}(s)=\frac{\hat{d}(s)}{\hat{v}_e(s)}=\frac{1}{V_{saw}} \quad (15)$$

Substituting (11), (12), and (15) into (10), the IVFF transfer function in buck mode can be derived as

$$G_{ff-buck}(s)=\frac{v_0}{v_0(1-S\frac{L_e}{R_{Ld}})}V_{saw} \quad (16)$$

Similarly, substituting (13)–(15) into (10), the IVFF transfer function in boost mode can be derived as

$$G_{ff-boost}(s)=\frac{1}{v_0(1-S\frac{L_e}{R_{Ld}})}V_{saw} \quad (17)$$

In (17), the term $sL_e/RL_d = sL_f\ V^2_o/RLdV^2_{\text{in-dc}}$ is a function of frequency, and the factor $L_e/RL_d = Lf\ V^2_o\ /RL_dV^2_{\text{in-dc}}$ reaches its maximum value at full load and minimum input voltage. According to the parameters of the prototype listed in Table I to appear in Section V, the magnitude of $sL_e\ /RL_d$ with the full load resistor RL_d = 21.6 Ω and the minimum input voltage $V_{\text{in-min}}$ = 250 V is depicted in Fig. 6. Fortunately, the input voltage of the battery-powered power supply [5], PFC application [9], RF amplifier supply [11], and fuel-cell power system [39] fluctuates at low frequency, and thus $|sL_e\ /RL_d|$ _ 1, as shown in Fig. 6. Therefore, (17) can be simplified as

$$G_{ff-boost}(s)=-\frac{1}{v_0}V_{saw} \quad (18)$$

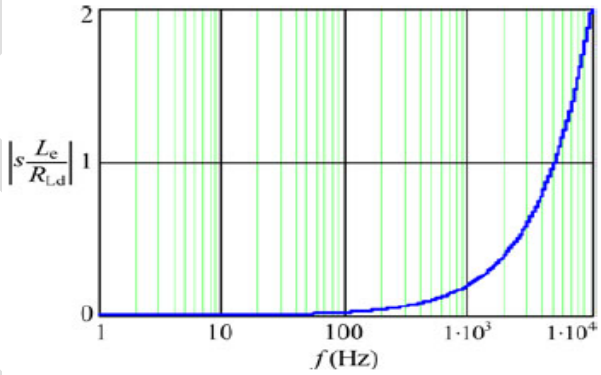

Fig. 6. Magnitude of *sLe /RLd* as the function of frequency

C. Two-Mode Control Scheme With IVFF Compensation

Since the TSBB converter can operate in buck and boost modes, and the IVFF transfer functions for the two operating modes are different, it is important to ensure that the TSBB converter operates in correct mode with correct IVFF transfer function and switches between the two modes automatically. According to (16) and (18), the output signals of the IVFF path under different operating modes can be expressed as

$$\begin{cases} v_{ff-buck} = G_{ff-buck}\,v_{in} = \frac{v_o}{v_{in-dc}^2}V_{saw}\,v_{in} \\ v_{ff-boost} = G_{ff-buck}\,v_{in} = -\frac{1}{v_o}V_{saw}\,v_{in} \end{cases} \quad (19)$$

As seen from (19), the ouput signal of the IVFF path in boost mode is independent of $V_{\text{in-dc}}$, so the value of $V_{\text{in-dc}}$ is considered only in the buck mode. If the value of $V_{\text{in-dc}}$ in $v_{\text{ff-buck}}$ is changed with the quiescent operation of the converter, a division operation on input voltage [33], [34], which requires rather complicated implementation, will be involved. For easy implementation, a tradeoff point, i.e., the middle value of the input voltage region in buck mode is set as $V_{\text{in-dc}}$, i.e., $V_{\text{in-dc}}$ = (360 + 500) / 2 = 430 V, in this paper. As seen in Fig. 5(b), the modulation signal *ve* is the sum of

the output signals of the IVFF path and the voltage regulator, i.e., $v_e = v_{ff} + v_{ea}$. Hence, according to (4) and (19), the modulation signals of the TSBB converter under the two-mode control scheme with IVFF compensation can be expressed as

$$\begin{cases} v_{e-buck} = v_{ff-buck} + v_{ea} + v_{bias} = -\frac{v_o V_{saw}}{v_{in-dc}^2} v_{in} + v_{ea} + v_{bias} \\ v_{e-boost} = v_{ff-boost} + v_{ea} = -\frac{V_{saw}}{v_o} v_{in} + v_{ea} \end{cases} \quad (20)$$

As discussed in Section II, the condition shown in (3), i.e., $v_{e\text{-buck}} - v_{e\text{-boost}} \geq V_{saw}$, should be satisfied for the proper two-mode operation. Substituting (20) into (3) leads to

$$v_{bias} \geq V_{saw} - v_o V_{saw} v_{in} \left(\frac{1}{v_0^2} - \frac{1}{v_{in-dc}^2}\right) \quad (21)$$

As mentioned earlier, $V_{\text{in-dc}}$ is set to the middle value of the input voltage region in buck mode, and it is greater than V_o .So, the right-hand side of (21) decreases with the input voltage

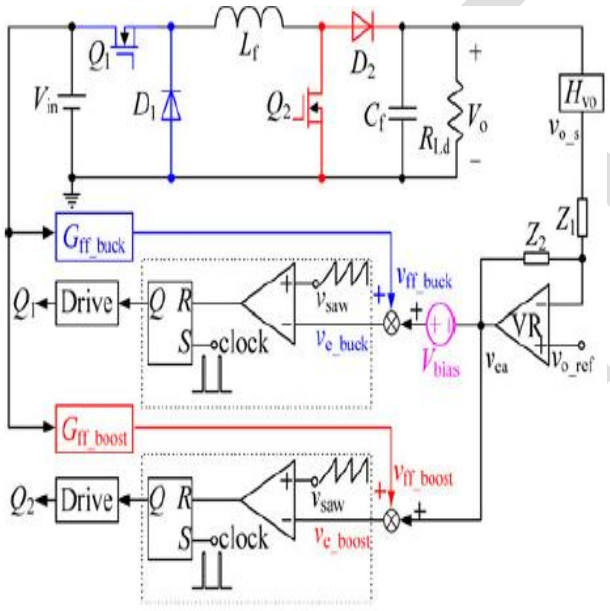

Fig. 7. Schematic diagram of the two-mode control scheme with IVFF.

V_{in} , and it gets its maximum value at the minimum input voltage $V_{\text{in-min}}$. So, here V_{bias} is set to this maximum value for ensuring smooth mode-switching between buck and boost modes with corresponding IVFF compensation as much as possible, i.e.,

$$v_{bias} = V_{saw} - v_o V_{saw} v_{in-min} \left(\frac{1}{v_0^2} - \frac{1}{v_{in-dc}^2}\right) \quad (22)$$

By substituting (22) into (20), the final modulation signals of the TSBB converter can be written as

$$\begin{cases} v_{e-buck} = v_{ff-buck} + v_{ea} + v_{bias} = -\frac{v_o}{v_{in-dc}^2} V_{saw} v_{in} + v_{ea} + v_{saw} - v_o V_{saw} v_{in-min} \\ v_{e-boost} = v_{ff-boost} + v_{ea} = -\frac{1}{v_o} V_{saw} v_{in} + v_{ea} \end{cases} \quad (23)$$

According to (23) and Table I, the value of $v_{e\text{-buck}} - v_{e\text{-boost}}$ at the mode-switching point is $1.09V_{saw}$, which can be treated as nearly smooth switching between buck and boost modes. Fig. 7 gives the schematic diagram of the two-mode control scheme with IVFF compensation, where $G_{\text{ff-buck}}$ and $G_{\text{ff-boost}}$ are the IVFF functions for buck and boost modes, expressed as (16) and (18), respectively, and V_{bias} is the dc bias voltage expressed as (22)

.

IV. COMPARISONS BETWEEN THE TWO-MODE CONTROL SCHEME WITH AND WITHOUT IVFF COMPENSATION

A. Output Signal of the Voltage Regulator

According to Fig. 3, the relationship between the modulation signal and the duty ratio under different operating modes can be expressed as

$$\begin{cases} \frac{v_{e-buck} - V_L}{d_1 T_s} = \frac{V_{saw}}{V_L}, v_{e-boost} < V_L (v_{in} \geq v_o) \\ \frac{v_{e-boost} - V_L}{d_2 T_s} v_{e-buck} < V_H (v_{in} < v_o) \end{cases} \quad (24)$$

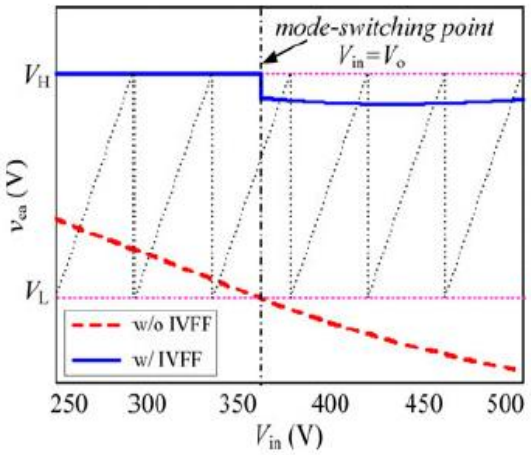

Fig. 8. Comparison of *v*ea between the two-mode control scheme with and without IVFF compensation.

Substituting the duty ratio expressions shown in (2) into (24) yields

$$\begin{cases} v_{e-buck} = \frac{V_0}{V_{in}} V_{saw} + V_L, v_{e-boost} < V_L (v_{in} \geq v_o) \\ v_{e-boost} = (1 - \frac{V_0}{V_{in}}) V_{saw} + V_L, v_{e-boost} < V_H (v_{in} < v_o) \end{cases} \quad (25)$$

It can be found from (25) that the modulation signals under the two-mode control scheme are the functions of only input voltage. After the input voltage being known, the corresponding modulation signal will be determined, no matter the IVFF compensation being incorporated or not. Combining (23) and (25), the output signal of the voltage regulator under the two-mode control scheme with IVFF compensation can be derived as

$$V_{ea}=\begin{cases} V_{saw}\left(\frac{V_0}{V_{in}}+\frac{v_o}{v_{in-dc}^2}v_{in}+\frac{v_{in-min}}{V_0}-\frac{v_o v_{in-min}}{v_{in-dc}^2}-1\right) \\ \quad +V_L(v_{in}\geq v_o) \\ V_H(v_{in}<v_o) \end{cases} \tag{26}$$

Similarly, combining (4) with $V_{bias} = V_{saw}$ and (25), the output signal of the voltage regulator under the two-mode control scheme without IVFF compensation can be derived as

$$V_{ea}=\begin{cases} \left(\frac{V_0}{V_{in}}-1\right)+V_{saw}+V_L(v_{in}\geq v_o) \\ \left(1-\frac{V_0}{V_{in}}\right)+V_{saw}+V_L(v_{in}<v_o) \end{cases} \tag{27}$$

According to (26), (27), and Table I, v_{ea} under the two-mode control scheme with and without IVFF compensation can be depicted, as the solid and dashed lines shown in Fig. 8, respectively. It can be seen that the variation of v_{ea} under the two-mode control scheme with IVFF compensation is much smaller than that without IVFF compensation over the entire input voltage range, which implies that the IVFF mainly regulated the output voltage, extremely alleviating the task of the voltage regulator and improving the transient response on the disturbance of the input voltage. Additionally, it also can be seen that v_{ea} has a small leap at the mode-switching point when the IVFF compensation is incorporated. This phenomenon is resulted from the introduction of IVFF compensation, leading to $v_{e\text{-buck}} - v_{e\text{-boost}} = 1.09V_{saw}$ at the mode-switching point, i.e., a nearly smooth switching between buck and boost modes, which has been discussed in Section III.

Substitution of (26) into (23) can obtain the modulation signals over the whole input voltage range for the TSBB converter under the two-mode control scheme with IVFF compensation, as shown in Fig. 9, which illustrates that automatic and nearly smooth mode-switching is achieved.

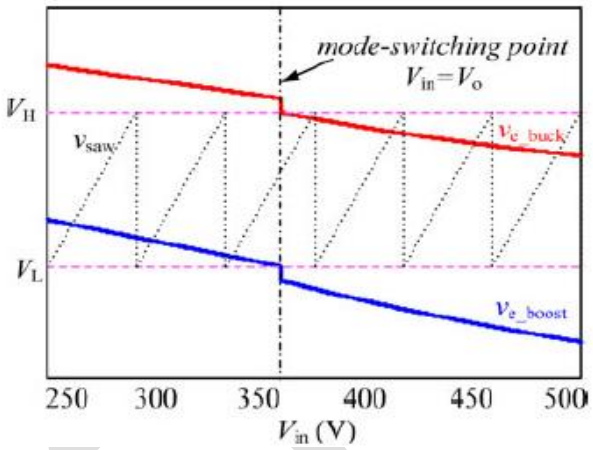

Fig. 9. Modulation signals under the two-mode control scheme with IVFF compensation.

B. Input-to-Output Voltage Transfer Function

According to Fig. 5, the loop gain of a dc–dc converter is Setting G_{vr} (s) = 1, and substituting $G_{vd\text{-buck}}(s)$ and $G_{vd\text{-boost}}(s)$ as described in (11) and (13) into (28) respectively, can obtain the uncompensated loop gains in buck and boost modes, which are defined as $T_{u\text{-buck}}(s)$ and $T_{u\text{-boost}}(s)$. According to Table I, the bode diagrams of $T_{u\text{-buck}}(s)$ at the maximum input voltage $V_{in\text{-max}}$ = 500 V and $T_{u\text{-boost}}(s)$ at the minimum input voltage $V_{in\text{-min}}$ = 250 V can be obtained, as the dashed lines shown in Fig. 10(a) and Fig. 10(b), respectively. Compared to $T_{u\text{-buck}}(s)$, $T_{u\text{-boost}}(s)$ presents a lower crossover frequency and smaller phase margin, due to the RHP zero. Therefore, the design of G_{vr} (s) is considered in boost mode.

Proportional-integral (PI) regulator is widely adopted as the voltage regulator. According to Fig. 10(b), $T_{u\text{-boost}}(s)$ has its maximum phase margin (PM) equaling 50° at 1 kHz. Given the negative phase-shift of PI regulator, the crossover frequency of the loop gain is set to be 1 kHz to ensure enough PM in boost mode. It means that the turning frequency of PI regulator needs to be far below 1 kHz, so the proportional component K_p that is mainly in effect at the crossover frequency and K_p = 30 is obtained. Then, by setting PM to 45°, the integral component K_i can be calculated as K_i = 100. On the other hand, considering the attenuation ability in high-frequency region of $T_{u\text{-boost}}$ is 0 dB, a pole with the slope of −20 dB is adopted, whose turning frequency is 10 kHz. So the voltage regulator can be expressed

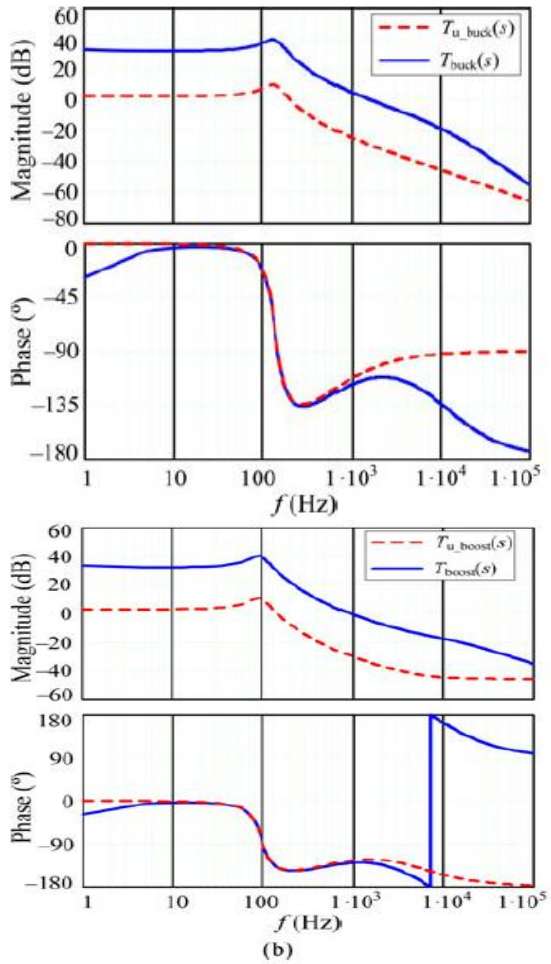

Fig. 10. Bode diagrams of the loop gains under different operating modes. (a) $V_{in\text{-}max}$ = 500 V, buck mode. (b) $V_{in\text{-}min}$ = 250 V, boost mode.

$$G_{vr}(s) = \frac{30s+100}{s\left(\frac{s}{1000}+1\right)} \quad (29)$$

In Fig. 10(a) and (b), the bode diagrams of the compensated loop gains in buck and boost modes, i.e., T_{buck} (s) and T_{boost}(s), are given with the solid lines, respectively. As seen, enough phase margins are ensured in both buck and boost modes. However, the bandwidths of the two modes are very low, leading to poor dynamic performance over the entire input voltage range. Therefore, it is very necessary to use the IVFF compensation to improve the input voltage transient response of the TSBB converter with the voltage regulator expressed in (29). According to Fig. 5, the closed-loop input-to-output voltage transfer function with IVFF compensation, $\Phi_{vo\text{-}v\,in}$, can be expressed as

$$\phi_{vo-vin}(s) = \frac{V_o(s)}{\hat{v}_{in}(s)} = \frac{G_{vo-vin}(s)+G_{ff}(s)G_{PWM}(s)G_{VD}(s)}{1+T(S)} \quad (30)$$

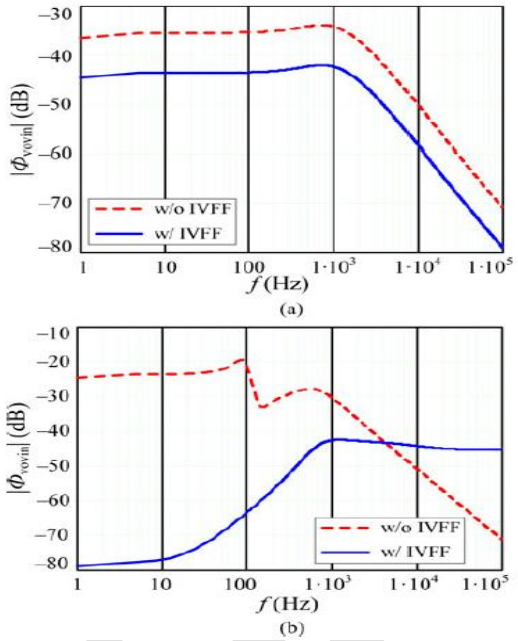

Fig. 11. Bode diagrams of the input to output voltage transfer function. (a) $V_{in\text{-}max}$ = 500 V, buck mode. (b) $V_{in\text{-}min}$ = 250 V, boost mode.

Substituting$G_{ff}(s)$,$G_{vo\text{-}vin}$ (s) and$G_{vd}(s)$ in buck and boost modes derived in Section III into (30), the magnitude of $\Phi_{vo\text{-}vin}$ with IVFF compensation in buck and boost modes can be obtained, shown with the solid lines in Fig. 11(a) and (b), respectively.

Likewise, the dashed lines in Fig. 11(a) and (b) are the magnitudes of $\Phi_{vo\text{-}vin}$ without IVFF compensation in buck and boost modes with G_{ff} (s) = 0, respectively. As seen, the ability on suppressing the effect of the input voltage disturbance on the output voltage for the TSBB converter with IVFF compensation is improved obviously, no matter in buck or boost mode. In addition, it also can be seen from Fig. 11 that the effect of the IVFF compensation in boost mode is more remarkable than that in buck mode in the low-frequency range. The reason is that the IVFF function in buck mode is not so accurate due to V_{in} dc equaling the middle value of the input voltage region of this mode, and the magnitude of the simplified IVFF function in boost mode is quite close to that without simplification in this frequency range, as described in (16)–(18).

V. INVERTING MODE OF OPERATION

The main feature of the voltage source inverter supply is that the inverter supplying DC voltage is nearly constant, relatively high capacitance capacitor energy storage is built in, to filter the transient load change. To achieve the field oriented control, the switching elements of the inverter constrain voltage to the motor

terminals with pulse width modulation control. The higher the switching frequency of the pulse width modulation, the faster and more punctual the achievable field oriented current vector control.

C.INDUCTION MOTOR

The induction motor has been known since almost the same time as the DC motor, but its role is increased only recently , since the drive technical features have been optimized and secured with inverter supply and field oriented control. The high power switching elements have enabled the development of the inverter technique, and high speed microcontrollers have enabled the development of the complicated control methods.

Field orientation control (FOC) of an induction motor can decouple its torque control from field control. This allows the motor to behave in the same manner as a separately excited dc motor. Extended speed range operation with constant power beyond base speed is accomplished by flux weakening. However, the presence of breakdown torque limits its extended constant power operation as shown in Fig.8.The advantage of the induction motor application prevails at *squirrel caged rotor motor* without slip-rings. Comparing with the commutated vehicle drives it possesses robust design, smaller space demand and do not need any maintenance. There are some attempts for water-cooled vehicle drive too.

V. simulation results

Simulink is a software package for modeling, simulating, and analyzing dynamical systems. It supports linear and nonlinear systems, modeled in continuous time, sampled time, or a hybrid of the two. Systems can be also multi-rate, i.e., have different parts that are sampled or updated at different rates. For modeling, Simulink provides a graphical user interface (GUI) for building models as block diagrams, using click-and-drag mouse operations. With this interface, you can draw the models just as you would with pencil and paper (or as most textbooks depict them).

This is a far cry from previous simulation packages that require you to formulate differential equations and difference equations in a language or program. Simulink includes a comprehensive blocklibrary of sinks, sources, linear and nonlinear components, and connectors. You can also customize and create your own blocks.

Models are hierarchical, so you can build models using both top-down and bottom-up approaches. You can view the system at a high-level, then double-click on blocks to go down through the levels to see increasing levels of model detail. This approach provides insight into how a model is organized and how its parts interact.

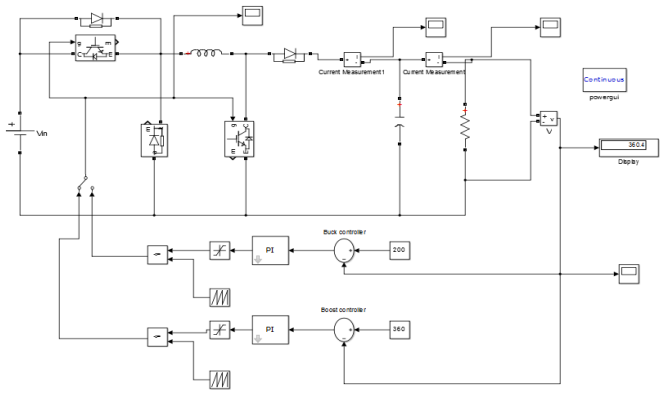

Fig.12. Boost/buck converter

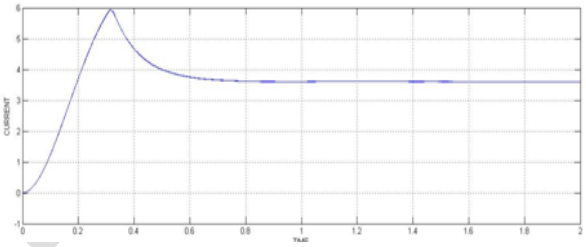

Fig.13. Boost current for converting mode

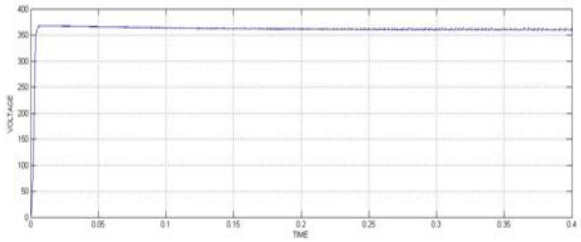

Fig.14. Boost voltage for converting mode

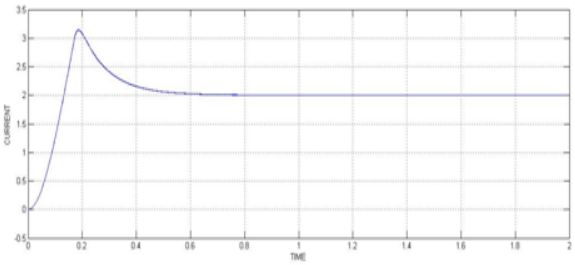

Fig.15. Buck current t for converting mode

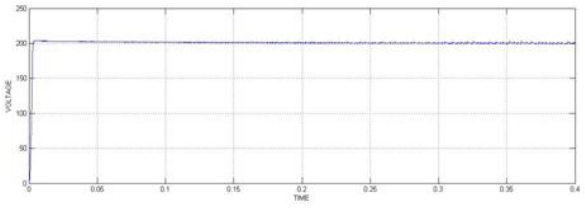

Fig.16. Buck voltage for converting mode

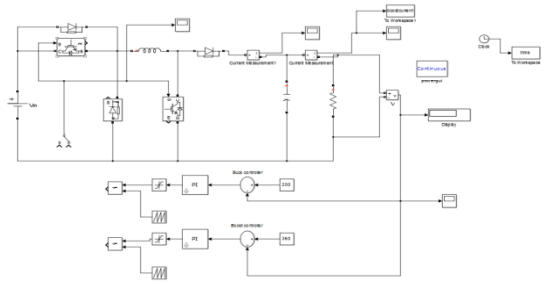

Fig.17. Boost/buck converter with out controller

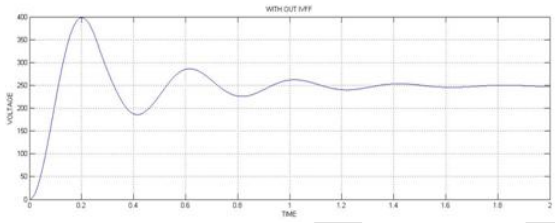

Fig.18. VOLTAGE for converting mode

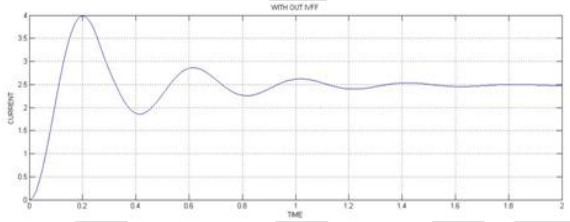

Fig.19. CURRENT for converting mode

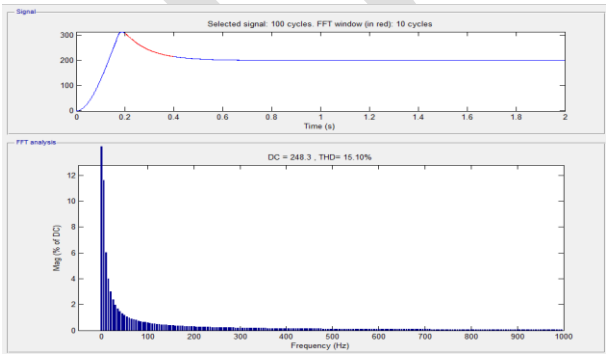

Fig.20. Fft analysis for buck boost converter with ivff.

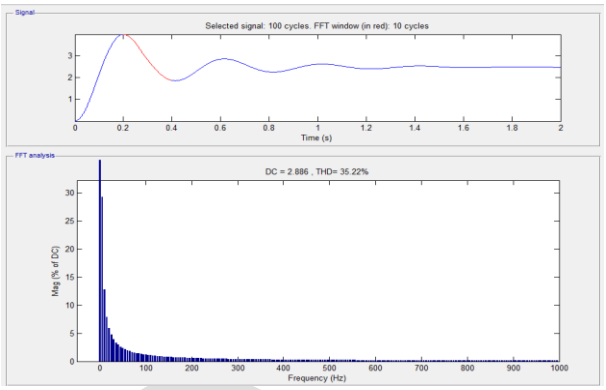

Fig.21. Fft analysis for buck boost converter without ivff

EXTENDED WORK OUTPUTS

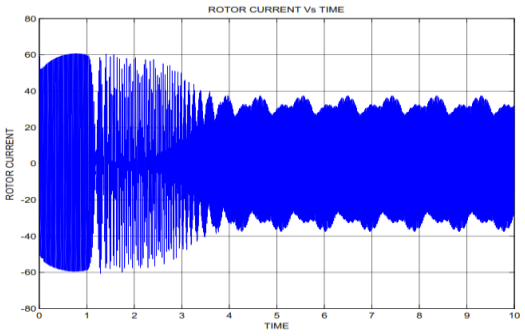

Fig.22.Rotor current for inverting mode

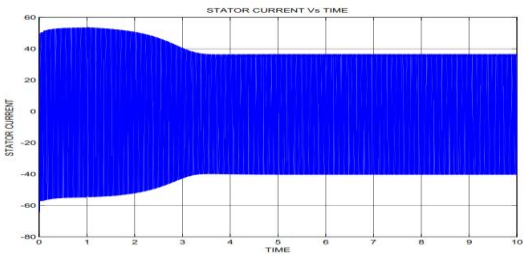

Fig.23.Stator current for inverting mode

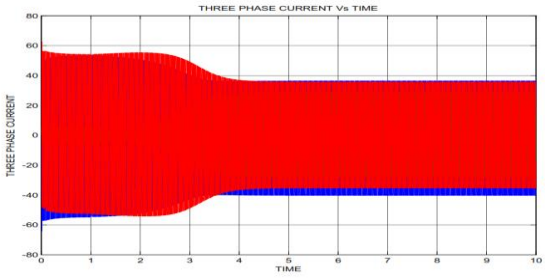

Fig.24.Three phase currentsfor inverting mode

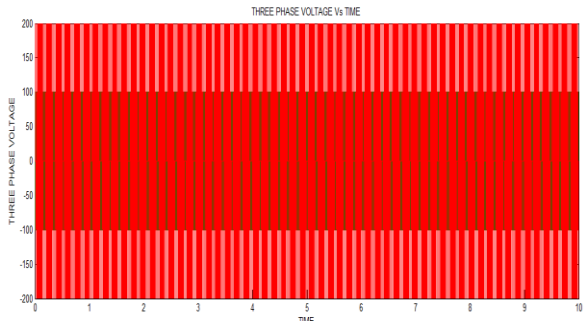

Fig.25.Three phase voltagesfor inverting mode

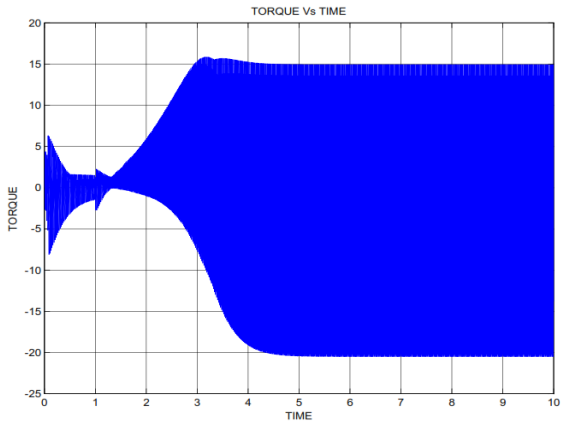

Fig.26.Torque for inverting mode

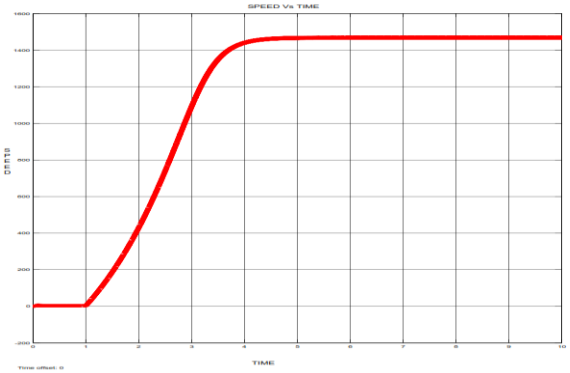

Fig.27.Speed for inverting mode

VI. CONCLUSION

So my present work is about the 250-500V input and 360V output and 6kw rated power prototype is designed to validate the effectiveness of the proposed control scheme in the matlab software and the results of the TSSB converter has an improved input transient response and more efficiency over a wide input range. My present work is extended by giving two switch buck boost converter (TSSB) to an inverter and then to an induction motor. So by varying the input voltage of an inverter we can vary the speed of an induction motor and the results for currents, speed and torque.is shown in my extension work.

REFERENCES

[1] R. W. Erickson and D. Maksimovic, *Fundamentals of Power Electronics*. Norwell, MA, USA: Kluwer, 2011.

[2] D. C. Jones and R. W. Erickson, "A nonlinear state machine for dead zone avoidance and mitigation in a synchronous noninverting buck-boost converter," *IEEE Trans. Power Electron.*, vol. 28, no. 1, pp. 467–480, Jan. 2013.

[3] C. Yao, X. Ruan, and X.Wang, "Isolated buck-boost dc/dc converters suitable for wide input-voltage range," *IEEE Trans. Power Electron.*, vol. 26, no. 9, pp. 2599–2613, Sep. 2011.

[4] X. Ren, X. Ruan, H. Qian, M. Li, and Q. Chen, "Three-mode dualfrequency two-edge modulation scheme for four-switch buck-boost converter," *IEEE Trans. Power Electron.*, vol. 24, no. 2, pp. 499–509, Feb. 2009.

[5] Y. J. Lee, A. Khaligh, A. Chakraborty, and A. Emadi, "A compensation technique for smooth transitions in a noninverting buck-boost converter," *IEEE Trans. Power Electron.*, vol. 24, no. 4, pp. 1002–1016, Apr. 2009.

[6] Y. J. Lee, A. Khaligh, A. Chakraborty, and A. Emadi, "Digital combination of buck and boost converters to control a positive buck-boost converter and improve the output transients," *IEEE Trans. Power Electron.*, vol. 24, no. 5, pp. 1267–1279, May 2009.

[7] E. Schaltz, P. O. Rasmussen, and A. Khaligh, "Non-inverting buck-boost converter for fuel cell application," in *Proc. IEEE Annual Conf. IEEE Ind. Electron.*, 2008, pp. 855–860.

[8] H. Qu, Y. Zhang, Y. Yao, and L. Wei, "Analysis of buck-boost converter for fuel cell electric vehicles," in *Proc. IEEE Int. Conf. Veh. Electron. Safety*, 2006, pp. 109–113.

[9] G. K. Andersen and F. Blaabjerg, "Current programmed control of a single-phase two-switch buck-boost power factor correction circuit," *IEEE Trans. Power Electron.*, vol. 53, no. 1, pp. 263–271, Feb. 2006.

[10] R. Morrison and M. G. Egan, "A new modulation strategy for a buckboost input ac/dc converter," *IEEE*

Trans. Power Electron., vol. 16, no. 1, pp. 34–45, Jan. 2001.

[11] B. Sahu and G. A. Rincon-Mora, "A high-efficiency linear RF power amplifier with a power-tracking dynamically adaptive buck-boost supply," *IEEE Trans. Microw. Theory Techniques*, vol. 52, no. 1, pp. 112–120, Jan. 2004.

[12] H. Liao, T. Liang, L. Yang, and J. Chen, "Non-inverting buck-boost converter with interleaved technique for fuel-cell system," *IET Power Electron.*, vol. 5, no. 8, pp. 1379–1388, 2012.

[13] R. Lin and R. Wang, "Non-inverting buck-boost power-factor-correction converter with wide input-voltage applications," in *Proc. IEEE Annual Conf. IEEE Ind. Electron.*, 2010, pp. T12-120–T12-124.

[14] T. Ishii, M. Yoshida, M. Motomori, and J. I. Hara, "Buck-boost converter," U.S. Patent 7 268 525, 2007.

[15] G. A. L. Henn, R. N. A. L. Silva, P. P. Prac¸a, L. H. S. C. Barreto, and D. S. Oliveira, Jr., "Interleaved-boost converter with high voltage gain," *IEEE Trans. Power Electron.*, vol. 25, no. 11, pp. 2753–2761, Nov. 2010.

[16] C. Yoon, J. Kim, and S. Choi, "Multiphase DC–DC converters using a boost-half-bridge cell for high-voltage and high-power applications," *IEEE Trans. Power Electron.*, vol. 26, no. 2, pp. 381–388, Feb. 2011.

[17] Y.-C. Hsieh, T.-C. Hsueh, and H.-C. Yen, "An interleavedboost converter with zero-voltage transition," *IEEE Trans.Power Electron.*, vol. 24, no. 4, pp. 973–978, Apr. 2009.

[18] X. Yang, Y. Ying, and W. Chen, "A novel interleaving control scheme for boost converters operating in critical conduction mode," *J. PowerElectron.*, vol. 10, no. 2, pp. 132–137, Mar. 2010.

[19] H. Xu, X. Wen, and L. Kong, "Dual-phase DC–DC converter in fuel cell electric vehicles," in *Proc. 9th IEEE Int. Power Electron. Congr.*, 2004, pp. 92–97.

[20] T. Reiter, D. Polenov, H. Probstle, and H-.G. Herzog, "PWM dead time op- timization method for automotive multiphase DC/DC-converters," *IEEE Trans. Power Electron.*, vol. 25, no. 6, pp. 1604–1614, Jun. 2010.